

Radiative B to tensor meson decays at NLO in SCET

Arslan Sikandar^{1 2}, M. Jamil Aslam

Department of Physics, Quaid-i-Azam University, Islamabad 45320, Pakistan.

Abstract

The radiative B to tensor ($K_2^*(1430)$, $f_2(1270)$, $a_2(1320)$) meson decays are studied at next-to-leading order (NLO) in soft-collinear effective theory (SCET). The SCET allows the systematic treatment of factorizable and non-factorizable contributions along with the resummation of large perturbative logarithms. We performed a two step matching and determined the soft-overlap function ζ_T^\perp and branching ratios for these B to tensor meson decays. In the case of $B \rightarrow K_2^*(1430)\gamma$, the numerical value of the branching ratio lies close to its experimental measurements. The estimated values of the branching ratios of CKM suppressed decays $B \rightarrow (a_2(1320), f_2(1270))\gamma$ are significant small compared to that of $B \rightarrow K_2^*(1430)\gamma$, but still could be measured in some ongoing and future B physics experiments.

1 Introduction

The weak B to pseudoscalar (P), vector (V), axial-vector (A) meson decays involving the quark level flavor changing neutral current transitions (FCNC) transitions $b \rightarrow (s, d)$, occur at loop level in the Standard Model (SM); therefore, these are suppressed both by the loop factors and the elements of Cabibbo-Kobayashi-Maskawa (CKM) matrix. This makes these FCNC transitions a fertile ground to hunt for the new physics (NP), i.e., physics beyond the SM (BSM). The radiative heavy-to-light, $B \rightarrow V\gamma$ decays are thus studied extensively, both within SM [1, 2, 3, 4] and in BSM approaches [5, 6]. Similar decay involving axial-vector meson in the final state, i.e., $B \rightarrow A\gamma$ is calculated in context of large-energy-effective theory (LEET) [7] and using soft-collinear effective theory (SCET) [8]. The radiative $B \rightarrow K_2^*(1430)$, where $K_2^*(1430)$ is a tensor mesons, is studied using perturbative QCD approach [9], light-cone sum rules [10, 11], Light front quark model (LFQM) [12, 13], Heavy Quark Effective Theory (HQET) [14], and LEET [15]. Also, the experimental averaged value of the branching ratio of $B \rightarrow K_2^*(1430)\gamma$ is measured to be $(1.24 \pm 0.24) \times 10^{-5}$ [16].

This study focuses the radiative B to tensor meson ($J^P = 2^+$) decays using the framework of SCET. The tensor mesons $K_2^*(1420)$, $a_2(1320)$, $f_2(1270)$ are lighter compared to B meson, and this justifies the use of SCET for the underlying $b \rightarrow (s, d)\gamma$ transition, where the masses of s and d -quarks are quite small compared to b -quark. The advantage of SCET is the ease it provides to study next-to-leading-order (NLO), i.e., ($\mathcal{O}(\alpha_s)$) corrections, power corrections and resummation. Moreover, SCET allows to divide systematically the heavy-to-light decay in terms of factorizable and non-factorizable contributions.

The SCET factorization for heavy-to-light decays at leading power in $1/m_b$ that is valid at all orders of $\mathcal{O}(\alpha_s)$ is

$$\langle T\gamma | Q_i | B \rangle = C_i^I \zeta_{B \rightarrow T} + \int_0^\infty \frac{d\omega}{\omega} \phi_B(\omega) \int_0^1 du \phi_T(u) C_i^{II}(\omega, u), \quad (1)$$

¹Current Address: Rudjer Boskovic Institute, Division of Theoretical Physics, Bijenička 54, HR-10000 Zagreb, Croatia.

²Corresponding Author

where C_i^I and C_i^{II} are Wilson Coefficients (WCs) containing the perturbative dynamics at hard scale ($\mu_Q \sim m_b$) and intermediate scale ($\mu_i \sim \sqrt{m_b \Lambda_{\text{QCD}}}$), respectively. ϕ_T and ϕ_B are light-cone distribution amplitude (LCDAs) of tensor and B mesons, respectively. $\zeta_{B \rightarrow T}$ is the soft form-factor, also called the soft-overlapping function at large recoil ($q^2 = 0$), accounts for the non-factorizable dynamics. The factorization Eq. (1) is required to correctly account the factorizable corrections in WCs [17, 18, 20, 19]. Using the SCET formalism with the factorization relation Eq. (1), we have to perform a two step matching procedure. In the first step QCD is matched onto SCET_I at hard scale μ_Q and later SCET_I is matched onto SCET_{II} at intermediate scale μ_i . This would require to introduce operators for the two effective theories using a power counting scheme. The introduction of these SCET operators make the resummation of the large logarithms possible. During this process, the resummation of C_i^I is avoided because of the hard scale, however, for the C_i^{II} it is performed due to lower value of the intermediate scale (for details: see [8]).

This scheme is motivated from the pioneering work done by Becher *et. al.* [21] for $B \rightarrow V\gamma$ decays, where the SCET treatment of this radiative decay at NLO in α_s and at leading power of $1/m_b$ has been done pedagogically. After introducing the relevant SCET operators, and taking the results of SCET_I anomalous dimensions from [22], the necessary matching calculations are performed. Later, using the calculation of SCET form factor for $B \rightarrow K^*\gamma$, its branching ratio is estimated [21]. Ref. [8] discussed the similar calculations for the radiative $B \rightarrow A\gamma$, where A is representing an axial-vector meson. In [23], the authors carried a study for the semileptonic $B \rightarrow K^*$ decay, i.e., $B \rightarrow K^*\ell^+\ell^-$ at NLO in α_s and leading power in $1/m_b$ expansion. Constraining the soft form factor, i.e., $\zeta_\perp(q^2 = 0)$ from the radiative $B \rightarrow K^*\gamma$ data, and using this together with the light-cone sum rules to determine the q^2 -dependence of $\zeta_\perp(q^2)$ the value of branching ratio is estimated in $q^2 = [1, 7]$ GeV range. Compared to the branching ratio of the semi-leptonic B -meson decays, the zero-position of the forward-backward asymmetry is less sensitive to different input parameters. In SM, its value is estimated to be $q_0^2 = (4.07_{-0.13}^{+0.16})$ [23].

The work is organized as follows: In Sect. 2, we define the relevant operators for $B \rightarrow T\gamma$ decay and discuss the momentum scaling. In Sect. 3, we work out the matching calculation from QCD to the SCET_I. In Sect. 4, the SCET_{II} operators are given as four-quark operators to match with the SCET_I operators and the relevant WCs, known as the jet-functions, are presented. These WCs are scale dependent and their evolution from hard to an intermediate scale involves the resummation, which we discuss in Sect. 5. We calculate the matrix elements for $B \rightarrow T\gamma$ in Sect. 6, and present the results for the branching ratios and compare them with some earlier results and the experimental measurements. Finally, Sect. 7 concludes of our main results.

2 SCET analysis of $B \rightarrow (K_2, f_2, a_2)\gamma$

In SM, the weak effective Hamiltonian (WEH) for the FCNC, $b \rightarrow (s, d)\gamma$, transitions is given by

$$\mathcal{H}_W = \frac{G_F}{\sqrt{2}} \sum_{p'=u,c} V_{p'p}^* V_{p'b} \sum_{i=1}^8 [C_i(\mu) Q_i(\mu)], \quad (2)$$

where $p = s$ for K_2^* and $p = d$ for (f_2, a_2) mesons. Utilizing the unitary relation and ignoring the loop contribution $V_{us(d)}^* V_{ub}$, which is doubly Cabibbo suppressed, we can write

$$\mathcal{H}_W = -\frac{G_F}{\sqrt{2}} \sum_{i=1}^8 V_{tp}^* V_{tb} [C_i(\mu) Q_i(\mu)]. \quad (3)$$

The WCs are known at next-to-next leading logarithm (NNLL) [24, 25, 26] while the four-quark operators are [27]:

$$\begin{aligned}
Q_1 &= (\bar{p}_L \gamma_\mu T^a c_L)(\bar{c}_L \gamma^\mu T^a b_L), & Q_2 &= (\bar{p}_L \gamma_\mu c_L)(\bar{c}_L \gamma^\mu b_L), \\
Q_3 &= (\bar{p}_L \gamma_\mu b_L) \sum_q (\bar{q} \gamma^\mu q), & Q_4 &= (\bar{p}_L \gamma_\mu T^a b_L) \sum_q (\bar{q} \gamma^\mu T^a q), \\
Q_5 &= (\bar{p}_L \gamma_\mu \gamma_\nu \gamma_\sigma b_L) \sum_q (\bar{q} \gamma^\mu \gamma^\nu \gamma^\sigma q), & Q_6 &= (\bar{p}_L \gamma_\mu \gamma_\nu \gamma_\sigma T^a b_L) \sum_q (\bar{q} \gamma^\mu \gamma^\nu \gamma^\sigma T^a q), \\
Q_7 &= \frac{e}{16\pi^2} m_b (\bar{p}_L \sigma^{\mu\nu} b_R) F_{\mu\nu}, & Q_8 &= \frac{g_s}{16\pi^2} m_b (\bar{p}_L \sigma^{\mu\nu} T^a b_R) G_{\mu\nu}^a.
\end{aligned} \tag{4}$$

In above equation, T^a is the $SU(3)$ color matrix, and m_b is the b -quark mass in $\overline{\text{MS}}$ scheme at momentum scale μ . The operator Q_2 contribute at α_s^2 , therefore, it is ignored for these NLO calculations. Also, the WCs for penguin operators $Q_3 - Q_6$ are too small, and hence we do not include their contributions in this work. The phenomenologically relevant operators for the radiative $B \rightarrow T\gamma$ decays at $\mathcal{O}(\alpha_s)$ are Q_1, Q_7 and Q_8 . Since the masses of these tensor mesons are around 1.5 GeV, which is about 3.5 times smaller than the mass of the B meson, they have a high collinear momentum at maximum recoil in these radiative decays. We assume that the outgoing meson is moving in a light-like direction with an associated vector n_μ . The velocity vector associated with the decaying B meson is v_μ , which is related to n_μ through an auxiliary light-like vector \bar{n}_μ as

$$\bar{n}^\mu = 2v^\mu - n^\mu, \tag{5}$$

satisfying $n^2 = \bar{n}^2 = 0$, $n \cdot \bar{n} = 2$, and correspondingly $v \cdot v = 1$. In $B \rightarrow T\gamma$ decay, the momenta of B , T , and γ are

$$p_B^\mu = m_B v^\mu, \quad p_T^\mu = E n^\mu + \frac{m_T^2}{4E} \bar{n}^\mu, \quad p_\gamma^\mu = \left(E - \frac{m_T^2}{4E}\right) \bar{n}^\mu, \tag{6}$$

here E is the off-shell energy [28] of the order $(m_B/2)$ while the momenta satisfy the on-shell conditions, i.e., $p_B^2 = m_B^2$, $p_T^2 = m_T^2$ and $p_\gamma^2 = 0$, respectively. This will help us to define the momenta of quarks and gluons according to different momentum regions in the heavy-quark limit, e.g., the soft region scales like $p_B - m_B v \sim \Lambda_{\text{QCD}}$. Generally, we decompose the momentum in terms of the light cone variables as

$$p^\mu = n \cdot p \frac{\bar{n}^\mu}{2} + \bar{n} \cdot p \frac{n^\mu}{2} + p_\perp^\mu = p_+^\mu + p_-^\mu + p_\perp^\mu, \tag{7}$$

where the different regions will thus have varying components of p_+^μ , p_-^μ and p_\perp^μ . Table 1 summarizes the regions and their scaling for different momentum labels, and we require them to satisfy the factorization relation given in Eq. (1) for these heavy to light radiative decays. The collinear region is further divided into n and \bar{n} -collinear regions, although the later do not appear for the radiative decays because $q^2 \equiv (p_B - p_T)^2 = p_\gamma^2 = 0$. Two more regions, i.e., hard and hard-collinear (again divided into n and \bar{n} - hard-collinear) are required to correctly reproduce the QCD infrared physics, manifested in the WCs \mathcal{C}^I and jet functions, respectively. Another possible mode is the soft-collinear mode, and this is interesting because the interaction of soft with a soft-collinear will yield a soft mode, while the interaction of collinear with soft-collinear will yield a collinear mode. However, the interaction of a soft with a collinear mode will yield a hard-collinear mode making the factorization relation unreliable. Therefore, to have the factorization valid, one has to show that up to any order in λ these modes do not contribute. Taking outgoing collinear quarks to be massless is also valid assumption for our case. Now, if the collinear quarks have a mass of order Λ_{QCD} , then the soft-collinear mode disappear - but in this case the soft and collinear propagators are not well-defined and require additional regulators. This may further require to prove factorization that is independent of these regulator, but it is not required in our case because $m_{s,d} < \Lambda_{\text{QCD}}$.

Table 1: Different momentum regions and their scaling that may appear in heavy-quark limit using the expansion parameter $\lambda \sim \Lambda_{\text{QCD}}/E$.

Label	Region	Scaling
Hard	(1,1,1)	m_b
Hard Collinear	$(\lambda, 1, \lambda^{1/2})$	$m_b \lambda^{1/2}$
Collinear	$(\lambda^2, 1, \lambda)$	$m_b \lambda$
Soft	$(\lambda, \lambda, \lambda)$	$m_b \lambda$
Soft-Collinear	$(\lambda^2, \lambda, \lambda^{3/2})$	$m_b \lambda^{3/2}$

3 QCD to SCET_I matching

The hard-collinear quark and gluon fields along with heavy-quark and soft fields scale as

$$\xi_{hc}, \xi_{hc}^- \sim \lambda^{1/2}, \quad A_{hc}^\mu \sim (\lambda, 1, \lambda^{1/2}), \quad h \sim \lambda^{3/2}, \quad A_s \sim (\lambda, \lambda, \lambda). \quad (8)$$

In Eq. (8), ξ , A^μ and h denote the quark, gluon and the heavy-quark fields, respectively. The subscripts hc , s and c represent the hard-collinear, soft and collinear modes, respectively. In SCET, the operators with derivatives of hard-collinear or collinear field are not suppressed for the larger momentum component and they can have same power counting. Therefore, to have gauge-invariant operators, the fields are connected by light-like Wilson's lines at different points, e.g., in SCET_I, the hard-collinear fields have to be invariant under hard-collinear gauge transformations, and this requires to introduce a hard-collinear Wilson line

$$W_{hc}(x) = \mathbb{P} \exp \left(ig \int_{-\infty}^0 ds_1 \bar{n} \cdot A_{hc}(x + s_1 \bar{n}) \right), \quad (9)$$

where the gauge-invariant hard-collinear fields are defined as

$$\begin{aligned} \chi_{hc}(x) &= W_{hc}^\dagger(x) \xi_{hc}(x) \\ \mathcal{A}_{hc}^\mu(x) &= W_{hc}^\dagger [i D_{hc}^\mu(x) W_{hc}(x)] + \frac{\bar{n}^\mu}{2} [W_{hc}^\dagger(x) g n \cdot A_s(x_-) W_{hc}(x) - g n \cdot A_s(x_-)]. \end{aligned} \quad (10)$$

In above equations, it can be noticed that the position variable, x , is defined as $x \equiv x_+ + x_- + x_\perp$ and s_1 is the light-ray variable in Eq. (9). The mass dimensions are used to construct the operators in SCET_I [21]. The simplest is the two-particle operator ($J^{\mathcal{A}}$) at dimension-3 while the higher power (subleading) three-particle operator ($J^{\mathcal{B}}$) has dimension-4. The \mathcal{A} -type operators are invariant under first re-parameterization condition that takes into account invariance under rescaling of the light-like vectors, i.e., $n^\mu \rightarrow (1 + \alpha)n^\mu$ and $\bar{n}^\mu \rightarrow (1 - \alpha)\bar{n}^\mu$. The operators are constructed using scalar ($\Gamma = I$), vector ($\Gamma_i = (\gamma^\mu, v^\mu, n^\mu)$), and tensor ($\Gamma_j = \gamma^{[\mu} \gamma^{\nu]}, \gamma^{[\mu} v^{\nu]}, \gamma^{[\mu} n^{\nu]}, v^{[\mu} n^{\nu]}$) Dirac structures, where square brackets denote the anti-commutation [21, 22, 30], and subscripts $i = 1, \dots, 3$ and $j = 1, \dots, 4$, correspond to three vector and four-tensor structures, respectively. Similarly, we can construct the \mathcal{B} -type operators, but since these are subleading, the Dirac structures required to be invariant under the second reparameterization condition allowing the light-like vectors to remain invariant in the perpendicular components, i.e., $n^\mu \rightarrow n^\mu + \epsilon_\perp^\mu$ and $\bar{n}^\mu \rightarrow \bar{n}^\mu - \epsilon_\perp^\mu$. This will mix the \mathcal{B} -type operators and one needs to define a new basis (for details see ref. [22]). In the change of basis, we now redefine the gamma matrices as $\gamma_\perp^\mu = \gamma^\mu - n^\mu \not{n}/2 - \bar{n}^\mu \not{\bar{n}}/2$. Thus, the new \mathcal{B}' -type operators could have the Dirac structure $\Gamma_i'^\mu = (\gamma_\perp^\mu, v^\mu, n^\mu)$ for vectors and $\Gamma_j'^{\mu\nu} = (\gamma_\perp^{[\mu} \gamma_\perp^{\nu]}, \gamma_\perp^{[\mu} v^{\nu]}, \gamma_\perp^{[\mu} n^{\nu]}, v^{[\mu} n^{\nu]})$ for tensors. The tree-level WCs for the two types (\mathcal{A} , \mathcal{B})

of operators introduced above are

$$\begin{aligned}
J_S^{\mathcal{A}} &= \bar{\chi}_{hc}(s_1 \bar{n}) h(0), & C_S^{\mathcal{A}} &= 1, \\
J_{V_i}^{\mathcal{A}} &= \bar{\chi}_{hc}(s_1 \bar{n}) \Gamma_i h(0), & C_{V_1}^{\mathcal{A}} &= 1, C_{V_2}^{\mathcal{A}} = 0, C_{V_3}^{\mathcal{A}} = 0, \\
J_S^{\mathcal{B}'} &= \bar{\chi}_{hc}(s_1 \bar{n}) \mathcal{A}_{\perp}(r \bar{n}) h(0), & C_S^{\mathcal{B}'} &= -1, \\
J_{V_i}^{\mathcal{B}'\mu} &= \bar{\chi}_{hc}(s_1 \bar{n}) \mathcal{A}_{\perp}(r \bar{n}) \Gamma_i^{\mu} h(0), & C_{V_1}^{\mathcal{B}'} &= 1, C_{V_2}^{\mathcal{B}'} = -2, C_{V_3}^{\mathcal{B}'} = 1 - z, \\
J_{V_4}^{\mathcal{B}'\mu} &= \bar{\chi}_{hc}(s_1 \bar{n}) \gamma_{\perp}^{\mu} \mathcal{A}_{\perp}(r \bar{n}) h(0), & C_{V_4}^{\mathcal{B}'} &= 0, \\
J_{T_j}^{\mathcal{B}'\mu} &= \bar{\chi}_{hc}(s_1 \bar{n}) \mathcal{A}_{\perp}(r \bar{n}) \Gamma_j^{\mu\nu} h(0), & C_{T_1}^{\mathcal{B}'} &= -1, C_{T_2}^{\mathcal{B}'} = -4, C_{T_3}^{\mathcal{B}'} = 2, C_{T_4}^{\mathcal{B}'} = 2, \\
J_{T_5}^{\mathcal{B}'\mu} &= \bar{\chi}_{hc}(s_1 \bar{n}) \mathcal{A}_{\perp\alpha}(r \bar{n}) \gamma_{\perp}^{[\alpha} \gamma_{\perp}^{\mu} \gamma_{\perp}^{\nu]} h(0), & C_{T_5}^{\mathcal{B}'} &= 0 \\
J_{T_6}^{\mathcal{B}'\mu} &= \bar{\chi}_{hc}(s_1 \bar{n}) v^{[\mu} \gamma_{\perp}^{\nu]} \mathcal{A}_{\perp}(r \bar{n}) h(0) & C_{T_6}^{\mathcal{B}'} &= 0, \\
J_{T_7}^{\mathcal{B}'\mu} &= \bar{\chi}_{hc}(s_1 \bar{n}) n^{[\mu} \gamma_{\perp}^{\nu]} \mathcal{A}_{\perp}(r \bar{n}) h(0), & C_{T_7}^{\mathcal{B}'} &= 2z.
\end{aligned} \tag{11}$$

The WCs for the corresponding pseudo-scalar and pseudo-tensor operators will remain the same, while those of the axial-vector currents will be

$$\begin{aligned}
J_{A_i}^{\mathcal{A}\mu} &= \bar{\chi}_{hc}(s_1 \bar{n}) \Gamma_i^{\mu} \gamma_5 h(0), & C_{A_1}^{\mathcal{A}} &= 1, C_{A_2}^{\mathcal{A}} = 0, C_{A_3}^{\mathcal{A}} = 0, \\
J_{A_i}^{\mathcal{B}'\mu} &= \bar{\chi}_{hc}(s_1 \bar{n}) \mathcal{A}_{\perp}(r \bar{n}) \Gamma_i^{\mu} \gamma_5 h(0), & C_{A_1}^{\mathcal{B}'} &= -1, C_{A_2}^{\mathcal{B}'} = -2, C_{A_3}^{\mathcal{B}'} = 1 - z, \\
J_{A_4}^{\mathcal{B}'\mu} &= \bar{\chi}_{hc}(s_1 \bar{n}) \gamma_{\perp}^{\mu} \gamma_5 \mathcal{A}_{\perp}(r \bar{n}) h(0), & C_{A_4}^{\mathcal{B}'} &= 0,
\end{aligned} \tag{12}$$

where $z = 2E/m_b$ with E being the energy of the final state quark. According to the factorization introduced in Eq. (1), the matching at leading power from QCD to SCET_I can be written as

$$\begin{aligned}
\mathcal{H}_{\text{eff}} \rightarrow & - \left(\int ds \int da \tilde{C}_i^{\mathcal{A}}(s) J_i^{\mathcal{A}}(s) \right. \\
& \left. + \sum_{j=1,2} \int ds \int dr \int da \tilde{C}_j^{\mathcal{B}'}(s, r, a) J_j^{\mathcal{B}'}(s, r, a) \right) + \dots
\end{aligned}$$

For different Dirac structures, the relevant operators for $b \rightarrow (s, d)\gamma$ decay at leading power in λ along with their WCs can be obtained from Eqs.(11) and (12). The \mathcal{A} -type operator and its WC is

$$\begin{aligned}
J_1^{\mathcal{A}}(s_1, a) &= \bar{\chi}_{hc}(s_1 \bar{n}) (1 + \gamma_5) \mathcal{A}_{hc\perp}^{(em)} h(0) \\
C^{\mathcal{A}}(E, E_{\gamma}) &= \int ds_1 \int da e^{is\bar{n}\cdot p} e^{ian\cdot p_{\gamma}} \tilde{C}^{\mathcal{A}}(s, a),
\end{aligned} \tag{13}$$

where $E = \bar{n} \cdot p/2$ and $E_{\gamma} \equiv n \cdot p_{\gamma}/2$. Also, $\bar{n} \cdot p$ is the large component of the total outgoing n -hard-collinear momentum and $n \cdot p_{\gamma}$ is the momentum of an outgoing photon. Similarly, the relevant SCET_I operators for \mathcal{B}' -type currents and their corresponding WCs are

$$J_1^{\mathcal{B}'}(s_1, r, a) = \bar{\chi}_{hc}(s_1 \bar{n}) (1 + \gamma_5) \mathcal{A}_{hc\perp}^{(em)}(an) \mathcal{A}_{hc\perp}(r \bar{n}) h(0) \tag{14}$$

$$J_2^{\mathcal{B}'}(s_1, r, a) = \bar{\chi}_{hc}(s_1 \bar{n}) (1 + \gamma_5) \mathcal{A}_{hc\perp}(r \bar{n}) \mathcal{A}_{hc\perp}^{(em)}(an) h(0) \tag{15}$$

$$C_j^{\mathcal{B}'}(E, E_{\gamma}, u) = \int ds_1 \int dr \int da e^{i(us_1 + \bar{u}r)\bar{n}\cdot p} e^{ian\cdot p_{\gamma}} \tilde{C}_j^{\mathcal{B}'}(s_1, r, a). \tag{16}$$

The index j in \mathcal{B}' -type WCs refer to the two types of operators represented by Eqs. (14) and Eq. (15). The variable $u(\bar{u})$ denotes the fraction of the large component of the n -hard-collinear momentum carried by the quark (gluon) field.

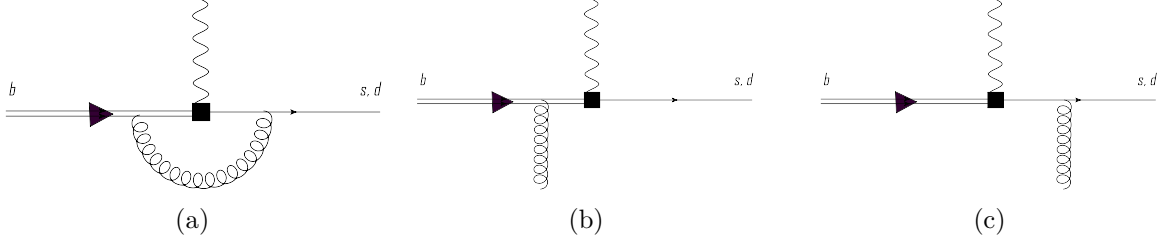


Figure 1: QCD diagrams for Q_7 operator matching onto $J^{\mathcal{A}}, J_1^{\mathcal{B}'}$ and $J_2^{\mathcal{B}'}$, respectively [8].

There could be a contribution from another set of diagrams with photon-emission from the spectator quark. The relevant SCET_I operator for these diagrams (\mathcal{C} -type matching) is a four-quark operator. Together with its WC, we can write

$$J^{\mathcal{C}}(s_1, r, a) = \bar{\chi}_{hc}(s_1 \bar{n})(1 + \gamma_5) \frac{\not{r}}{2} \chi_{hc}(r \bar{n}) \bar{\chi}_{\bar{h}\bar{c}}(an)(1 + \gamma_5) \frac{\not{a}}{2} h(0)$$

$$C_k^{\mathcal{C}}(u) = \int ds_1 \int dr \int da e^{i(us_1 + \bar{u}r) \bar{n} \cdot p} e^{ian \cdot p \gamma} \tilde{C}_k^{\mathcal{C}}(s_1, r, a). \quad (17)$$

The matching calculation at an order of α_s for \mathcal{A} -type operator is a loop diagram while for \mathcal{B}' -type it is at a tree level. Let us denote $\Delta_i C_j^{(\mathcal{A}, \mathcal{B}', \mathcal{C})}$ as the matching result of weak effective operators Q_i to the SCET_I operators $J_j^{\mathcal{A}, \mathcal{B}', \mathcal{C}}$, and write the total matching coefficients as

$$\mathcal{C}^{\mathcal{A}} = \frac{G_F}{\sqrt{2}} \sum_{p=u,c} V_{ps}^* V_{pb} \left[C_1(\mu_Q) \Delta_1^p C^{\mathcal{A}}(\mu_Q, \mu) + C_7(\mu_Q) \Delta_7 C^{\mathcal{A}}(\mu_Q, \mu) + C_8(\mu_Q) \Delta_8 C^{\mathcal{A}}(\mu_Q, \mu) \right],$$

$$\mathcal{C}^{\mathcal{B}' } = \frac{G_F}{\sqrt{2}} \sum_{p=u,c} V_{ps}^* V_{pb} \left[C_1(\mu_Q) \Delta_1^p C_{1,2}^{\mathcal{B}' }(\mu_Q, \mu) + C_7(\mu_Q) \Delta_7 C_{1,2}^{\mathcal{B}' }(\mu_Q, \mu) + C_8(\mu_Q) \Delta_8 C_{1,2}^{\mathcal{B}' }(\mu_Q, \mu) \right],$$

$$\mathcal{C}^{\mathcal{C}} = \frac{G_F}{\sqrt{2}} \sum_{p=u,c} V_{ps}^* V_{pb} \left[C_1(\mu_Q) \Delta_1^p C^{\mathcal{C}}(\mu_Q, \mu) + C_7(\mu_Q) \Delta_7 C^{\mathcal{C}}(\mu_Q, \mu) + C_8(\mu_Q) \Delta_8 C^{\mathcal{C}}(\mu_Q, \mu) \right]. \quad (18)$$

Here μ_Q is the scale at which QCD is matched to SCET_I and μ is the renormalization scale in the effective theory. The matching of Q_7 is performed at loop-level (Fig1a) for \mathcal{A} -type ($J^{\mathcal{A}}$) and at tree-level (Fig(1b,1c)) for \mathcal{B} -type ($J^{\mathcal{B}'}$) operators [30, 32, 31]:

$$\Delta_7 C^{\mathcal{A}} = \frac{e \bar{m}_b E \gamma}{2\pi^2} \left\{ 1 + \frac{\alpha_s(m_b) C_F}{4\pi} \left[-2\ln^2 \frac{\mu}{2E} - 5\ln \frac{\mu}{2E} - 2\ln \frac{\mu_{QCD}}{2E} - 2\text{Li}_2\left(1 - \frac{2E}{m_b}\right) - 6 - \frac{\pi^2}{12} \right] \right\},$$

$$\Delta_7 C_1^{\mathcal{B}' } = \frac{e \bar{m}_b E \gamma}{4\pi^2 m_b},$$

$$\Delta_7 C_2^{\mathcal{B}' } = 0. \quad (19)$$

Here \bar{m}_b is the b -quark mass at next-to-leading order, i.e.,

$$\bar{m}_b = m_b \left[1 + \frac{\alpha_s(\mu) C_F}{4\pi} \left(3\ln \frac{m_b^2}{\mu^2} - 4 \right) \right].$$

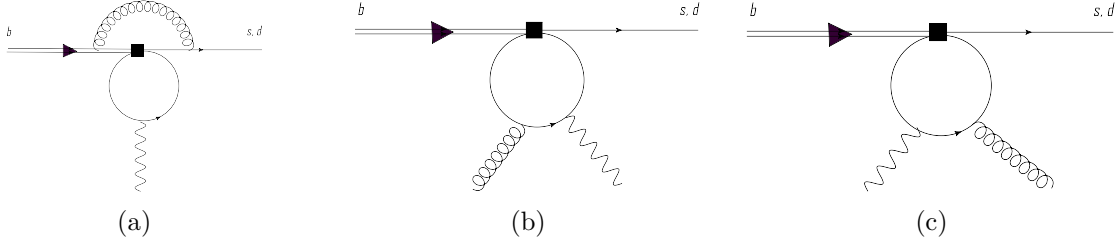


Figure 2: QCD diagrams for Q_1 operator matching onto $J^{\mathcal{A}}, J_1^{\mathcal{B}'}$ and $J_2^{\mathcal{B}'}$, respectively [8].

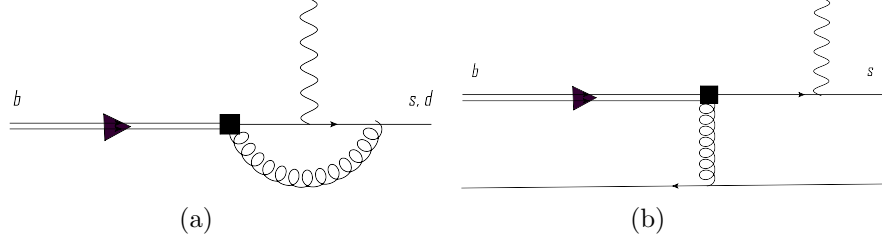


Figure 3: QCD diagrams for Q_8 operator matching onto $J^{\mathcal{A}}, J_1^{\mathcal{B}'}$ and $J_2^{\mathcal{B}'}$, respectively [8].

The matching of Q_1 operator with a charm quark loop (setting $m_u = 0$) for \mathcal{A} -type matching (Fig (2a)), and \mathcal{B}' -type matching (Fig (2b,2c)) give the following WCs

$$\begin{aligned}\Delta_1 C^{\mathcal{A}} &= \frac{\alpha_s C_F}{4\pi} G_i(x_c) \Delta_7 C^{\mathcal{A}}, \\ \Delta_1 C_1^{\mathcal{B}'}(u) &= -\Delta_1^q C_2^{\mathcal{B}'}(u) = \frac{2e}{3} f\left(\frac{\bar{m}_c^2}{4\bar{u}EE_\gamma}\right) \Delta_7 C_1^{\mathcal{B}'},\end{aligned}\quad (20)$$

where $x_c = \bar{m}_c^2/m_b^2$ and the functions $G_1(x_c)$ and $f\left(\frac{\bar{m}_c^2}{4\bar{u}EE_\gamma}\right)$ are given in Appendix.

The relevant diagrams for matching the chromomagnetic operator Q_8 to SCET_I \mathcal{A} - and \mathcal{B}' -types operators are given in Figs. 3a and 3b, respectively. The diagrams where a photon is emitted from the b -quark for Q_8 operator are suppressed. The WCs thus found are [33]:

$$\begin{aligned}\Delta_8 C^{\mathcal{A}} &= \frac{\alpha_s C_F}{4\pi} G_8 \Delta_7 C^{\mathcal{A}}, \\ \Delta_8 C_1^{\mathcal{B}'}(u) &= \frac{\bar{m}_b}{4\pi^2} \frac{e}{3} \frac{\bar{u}}{u}, \\ \Delta_8 C_2^{\mathcal{B}'}(u) &= 0.\end{aligned}\quad (21)$$

There are a few other diagrams in which the photon can be emitted but they are power suppressed. One such diagram is the photon emission from b -quark for Q_1 matching onto $J^{\mathcal{A}}$. Another is the photon emission from the outgoing spectator quark which is also power-suppressed [34, 35]. Although the photon emission from incoming soft-spectator quark are eventually not power suppressed when matched to SCET_{II}, but they vanish when the matrix elements are calculated for the transversely polarized tensor meson.

4 SCET_{II} Operators and SCET_I \rightarrow SCET_{II} matching

In the two step matching procedure, the next step is to match the intermediate theory SCET_I to the final theory SCET_{II} to find the corresponding WCs, which are also known as the jet functions.

To start with, let us define the gauge-invariant fields required for SCET_{II}, i.e.,

$$\begin{aligned}\bar{\chi}_c &= \mathcal{W}_c^\dagger \xi_c \sim \lambda, & Q_s &= \mathcal{S}^\dagger q_s \sim \lambda^{3/2}, & \mathcal{H} &= \mathcal{S}^\dagger h \sim \lambda^{3/2} \\ \mathcal{A}_c^\mu &= \mathcal{W}_c^\dagger (iD_c^\mu \mathcal{W}_c) \sim (\lambda^2, 0, \lambda), & \mathcal{A}_s^\mu &= \mathcal{S}^\dagger (iD_s^\mu \mathcal{S}) \sim (\lambda^2, 0, \lambda).\end{aligned}\quad (22)$$

Here the gauge-invariant operators are constructed using the soft and collinear Wilson lines

$$\begin{aligned}\mathcal{W}_c(x) &= \mathbb{P} \exp \left(ig \int_{-\infty}^0 ds_1 \bar{n} \cdot A_c(x + s_1 \bar{n}) \right) \\ \mathcal{S}(x) &= \mathbb{P} \exp \left(ig \int_{-\infty}^0 ds_1 \bar{n} \cdot A_s(x + s_1 \bar{n}) \right).\end{aligned}\quad (23)$$

The non-factorizable part (soft-overlap function) can be defined as the matrix elements of $J^{\mathcal{A}}$ operators, therefore, the \mathcal{A} -type matching of SCET_I to SCET_{II} is not required. For \mathcal{B}' -type matching, the SCET_{II} operators at tree level can be defined as

$$\begin{aligned}O_1^{\mathcal{B}'}(s_1, t) &= \bar{\chi}_c(s_1 \bar{n})(1 + \gamma_5) \mathcal{A}_{c\perp}^{(em)}(0) \frac{\bar{\eta}}{2} \chi_c(0) \bar{Q}_s(tn)(1 - \gamma_5) \frac{\eta}{2} \mathcal{H}_s(0) \\ O_2^{\mathcal{B}'}(s_1, t) &= \bar{\chi}_c(s_1 \bar{n})(1 + \gamma_5) \frac{\bar{\eta}}{2} \chi_c(0) \bar{Q}_s(tn)(1 + \gamma_5) \frac{\eta}{2} \mathcal{A}_{c\perp}^{(em)}(0) \mathcal{H}_s(0).\end{aligned}\quad (24)$$

From Eq. (24), one can notice that the leading power operators have a collinear and soft part. Thus in SCET_{II}, the matrix elements for $B \rightarrow T$ can be written in terms of the LCDAs, independently for soft B and collinear tensor mesons. This decoupling into soft and collinear parts prevented end-point divergences to appear in the convolution integrals of Eq. (1). The corresponding WC in momentum space is given as

$$D_{1,2}^{\mathcal{B}'}(\omega, u) \equiv \int ds_1 \int dt e^{-i\omega n \cdot vt} e^{ius_1 \bar{n} \cdot p} \tilde{D}_{1,2}^{\mathcal{B}'}(s_1, t), \quad (25)$$

which is a convolution of the SCET_I WC C_i^B , with a jet function $\mathcal{J}_{\perp, \parallel}$, i.e.,

$$D_{1,2}^{\mathcal{B}'}(\omega, u, \mu_i) = \frac{1}{\omega} \int_0^1 dy \mathcal{J}_\perp \left(u, y, \ln \frac{2E\omega}{\mu_i^2}, \mu_i \right) C_{1,2}^{\mathcal{B}'}(y, \mu_1), \quad (26)$$

where $\mu_i \sim \sqrt{2E\Lambda_{QCD}}$ is an intermediate scale. At tree level, the matching of $J_1^{\mathcal{B}'}$ onto $O_1^{\mathcal{B}'}$ is trivial (c.f. Fig. 4) and the corresponding jet function is given as

$$\mathcal{J}_\perp(u, v) = \mathcal{J}_\parallel(u, v) = -\frac{4\pi C_F \alpha_s}{N} \frac{1}{2E\bar{u}} \delta(u - v) \quad (27)$$

while the similar matching for $J_2^{\mathcal{B}'}$ is suppressed at a leading power.

5 Resummation

In the matching calculations of previous sections, we introduced two scales, i.e., the hard scale $\mu_Q \sim m_b$ at which we matched QCD to SCET_I and intermediate scale $\mu_i \sim \sqrt{2E\Lambda_{QCD}}$ at which SCET_I is matched to SCET_{II}. To evolve the matching coefficients from a higher to a lower scale, we are required to solve the renormalization group (RG) equation for SCET_I operators. In this context, since only the hard scale μ_Q is involved in the matching calculations for the \mathcal{A} -type operators, we may choose the dependence of soft overlap function on μ_Q , which help us to avoid the RG evolution of \mathcal{A} -type operators. For the \mathcal{B}' -type operators, the evolution of scale requires

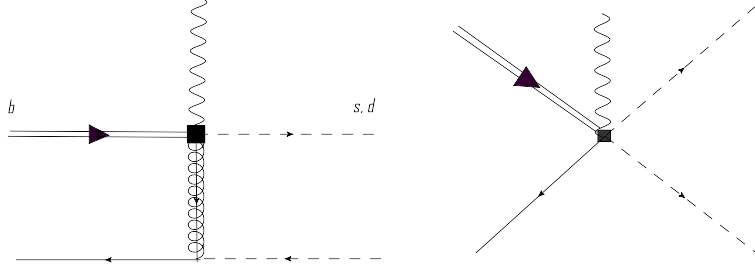


Figure 4: SCET_I diagram matching onto SCET_{II} 4-quark operator. The dashed gluon is hard-collinear[8].

the calculation of the one-loop anomalous dimension by keeping the UV divergent terms appearing in SCET_I loop diagrams (c.f. Fig. 3 of [22]).

The evolution of the \mathcal{B}' -type coefficients read as [15]

$$\frac{d}{d\ln\mu} \mathcal{C}_j^{\mathcal{B}'}(E, v) = \gamma_{ij}^{\mathcal{B}'}(u, v) \mathcal{C}_i^{\mathcal{B}'}(E, u), \quad (28)$$

where $\gamma^{\mathcal{B}'}$ is the corresponding anomalous dimension. The solution of the evolution equation (28) is

$$\mathcal{C}_j^{\mathcal{B}'}(E, u, \mu) = \left(\frac{2E}{\mu_Q} \right)^{a(\mu_Q, \mu)} e^{S(\mu_Q, \mu)} \int_0^1 dv U_{\perp, \parallel}(u, v, \mu_Q, \mu) \mathcal{C}_j^{\mathcal{B}'}(E, v, \mu_Q). \quad (29)$$

Here prime notation is adopted to make it consistent with our earlier tree level coefficients in Eq. (11). The functions $a(\mu_Q, \mu)$ and $S(\mu_Q, \mu)$ appeared in Eq. (29) are defined as [36]

$$\begin{aligned} S(\mu_Q, \mu) &= \frac{\Gamma_0}{4\beta_0^2} \left[\frac{4\pi}{\alpha_s(\mu_Q)} \left(1 - \frac{1}{r_1} - \ln r_1 \right) + \frac{\beta_1}{2\beta_0} \ln^2 r_1 - \left(\frac{\Gamma_1}{\Gamma_0} - \frac{\beta_1}{\beta_0} (r_1 - 1 - \ln r_1) \right) \right] \\ a(\mu_Q, \mu) &= -\frac{\Gamma_0}{2\beta_0} \ln r_1, \end{aligned} \quad (30)$$

where $\Gamma_0 = 4C_F$ and

$$\begin{aligned} \Gamma_1 &= 4C_F \left[\left(\frac{67}{9} - \frac{\pi^2}{3} \right) C_A - \frac{20}{9} T_F n_f \right], \\ \beta_0 &= \frac{11}{3} C_A - \frac{4}{3} T_F n_F \\ \beta_1 &= \frac{34}{3} C_A^2 - \frac{20}{3} C_A T_F n_f - 4C_F T_F n_f, \\ r_1 &= \alpha_s(\mu) / \alpha_s(\mu_Q). \end{aligned} \quad (31)$$

To find the evolution kernels $U_{\perp, \parallel}$, we employed the method used in [22] to solve the RG equation. Using the initial condition $U_{\perp, \parallel}(u, v, \mu_Q, \mu_Q) = \delta(u - v)$, we have

$$\frac{d}{d\ln\mu} \frac{U_{\perp, \parallel}(u, v, \mu_Q, \mu)}{\bar{u}} = \int_0^1 dy y \bar{y}^2 \frac{V_{\perp, \parallel}}{\bar{y} \bar{u}} \frac{U_{\perp, \parallel}(u, v, \mu_Q, \mu)}{\bar{y}} + w(u) \frac{U_{\perp, \parallel}(u, v, \mu_Q, \mu)}{\bar{u}}. \quad (32)$$

The functions $V_{\perp, \parallel}$ and $w(u)$ are defined in [22] which are the anomalous dimension contributions. A basis function comprising of Jacobi Polynomials (obtained by solving eigenvalue equation for

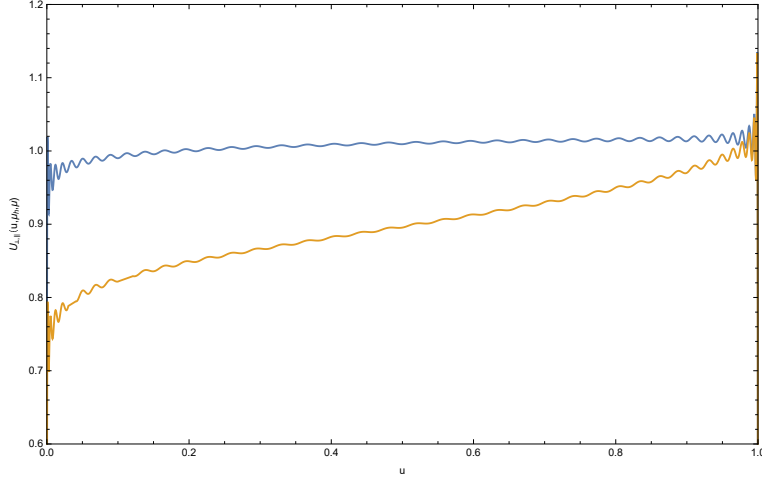


Figure 5: Evolution function with blue being U_{\parallel} and orange being U_{\perp} using 80 basis functions.

$V_{\perp,\parallel}$) is used to construct the solution for Eq. (32). This solution is plotted in Fig. 5 by taking a set of 80 basis functions. In the case of radiative decays, the perpendicular evolution function U_{\perp} is important.³

6 Matrix elements and Branching Ratios

Let $p_B^{\mu}(p_T^{\mu})$ and $m_B(m_T)$ are the momentum and mass of $B(T)$ meson, respectively. The polarization of the spin-2 meson can be written as $\varepsilon_{\mu\nu}(\lambda)$, with λ representing the helicity. The polarization tensor satisfying $\varepsilon_{\mu\nu}(\lambda)p_T^{\nu} = 0$ is traceless and symmetric. Hence, it is easy to construct it from the polarization states of a massive vector (spin-1) particle, i.e.,

$$\begin{aligned}\varepsilon_{\mu\nu}(\pm 2) &= \varepsilon(\pm)_{\mu}\varepsilon(\pm)_{\nu}, \\ \varepsilon_{\mu\nu}(\pm 1) &= \sqrt{\frac{1}{2}}(\varepsilon(\pm)_{\mu}\varepsilon(0)_{\nu} + \varepsilon(0)_{\mu}\varepsilon(\pm)_{\nu}), \\ \varepsilon_{\mu\nu}(\pm 0) &= \sqrt{\frac{1}{6}}(\varepsilon(+)_{\mu}\varepsilon(-)_{\nu} + \varepsilon(-)_{\mu}\varepsilon(+)_{\nu}) + \sqrt{\frac{2}{3}}\varepsilon(0)_{\mu}\varepsilon(0)_{\nu}.\end{aligned}\tag{33}$$

Here, the massive vector states $\varepsilon_{\mu}(\pm)$ and $\varepsilon_{\mu}(0)$ are given as;

$$\begin{aligned}\varepsilon_{\mu}(0) &= \left(\frac{|\vec{p}_T|}{m_T}, 0, 0, \frac{E_F}{m_T}\right), \\ \varepsilon_{\mu}(\pm) &= \frac{1}{\sqrt{2}}(0, \mp 1, -i, 0).\end{aligned}\tag{34}$$

Here $E_F = \frac{m_B^2 + m_T^2}{2m_B}$ is the energy of the final state tensor meson. At the maximum recoil, its value is $E_F \sim E = m_B/2$, while its 3-momentum is, $|\vec{p}_T| = \sqrt{E_F^2 - m_B^2}$. It is useful to introduce a new polarization vector $\varepsilon_{\perp\mu}$

$$\varepsilon_{\perp\mu}(\lambda) = \varepsilon_{\mu\nu}(\lambda)\frac{p_T^{\nu}}{m_B},\tag{35}$$

³In our previous paper [8], the perpendicular and parallel components were mistakenly interchanged in the text.

Input Values					
m_B	5.28 GeV	$m_b(\bar{m}_b)[37]$	4.18 GeV	$\tau_B[16]$	1.519 ps
$m_{K_2^*}$	1.43 GeV	m_{f_2}	1.27 GeV	m_{a_2}	1.32 GeV
$f_{K_2^*}^\perp(1\text{GeV})[10]$	0.077 ± 0.014 GeV	$f_{f_2}^\perp(1\text{GeV})[10]$	0.117 ± 0.025 GeV	$f_{a_2}^\perp(1\text{GeV})[10]$	0.105 ± 0.021 GeV
$f_B[37]$	0.190 GeV	G_F	1.16×10^{-6} GeV	$ V_{cd}^* V_{cs} $	0.0088
$ V_{cs}^* V_{cb} $	4×10^{-2}	$a_{1\perp}^T(1\text{GeV})$	5/3	$a_{1\parallel}^T(1\text{GeV})$	5/3

Table 2: The values of input parameters used in the numerical analysis.

such that $\varepsilon_{\perp\mu}(\pm 2) = 0$, $\varepsilon_{\perp\mu}(\pm 1) = (|\vec{p}_T|/m_B)\beta_{\perp}\varepsilon_{\mu}(\pm)$, $\varepsilon_{\perp\mu}(\pm 0) = (|\vec{p}_T|/m_B)\alpha_L\varepsilon_{\mu}(0)$ with $\beta_{\perp} = \sqrt{1/2}$, and $\alpha_L = \sqrt{2/3}$. Using the transversality condition $\varepsilon_{\perp}^* \cdot p_T = 0$ gives

$$\varepsilon_{\perp}^* \cdot n = -\frac{m_T^2}{4E|\vec{p}_T|}\varepsilon_{\perp}^* \cdot \bar{n}. \quad (36)$$

The photon has polarization ϵ^* and for the real photon $\epsilon^* \cdot p_{\gamma} = \epsilon^* \cdot \bar{n} = 0$. The $B \rightarrow T$ form factors can be parameterized in terms of soft-overlap function ζ_T^\perp by using SCET_I \mathcal{A} -type operator

$$\langle T(p_T) | \bar{\chi}_{hc} \Gamma h | B(v) \rangle = -2E_F \zeta_T^\perp(E_F) \text{tr}[\bar{\mathcal{M}}_{T\perp}(n) \Gamma \mathcal{M}_B(v)], \quad (37)$$

where the projection operators, $\mathcal{M}_{T\perp}(n)$ and $\mathcal{M}_B(v)$ read as

$$\mathcal{M}_B(v) = -\frac{1+\not{v}}{2}\gamma_5, \quad \bar{\mathcal{M}}_{T\perp}(n) = \not{\varepsilon}_{\perp}^* \frac{\not{n}\not{v}}{4}. \quad (38)$$

This results in

$$\langle T\gamma | J^{\mathcal{A}} | B \rangle = 4\mathcal{C}^{\mathcal{A}} E_F \left(1 + \frac{m_T^2}{8E_F|\vec{p}_T|} \right) \zeta_T^\perp(E_F). \quad (39)$$

The matrix elements of \mathcal{B}' -type currents $O_{1,2}^{\mathcal{B}'}$ of SCET_{II}, with independent soft and collinear parts can be written as a convolution of the LCDA's of the respective meson. We can write it as

$$\langle 0 | \bar{Q}_s(tn) \frac{\not{n}}{2} \Gamma \mathcal{H}(0) | \bar{B}(v) \rangle = -\frac{i\sqrt{m_B}F(\mu)}{2} \text{Tr} \left(\frac{\not{n}}{2} \Gamma \frac{1+\not{v}}{2} \gamma_5 \right) \times \int_0^\infty d\omega e^{-i\omega tn \cdot v} \phi_B(\omega, \mu, \quad (40)$$

$$\langle T_\perp(p_F, \eta^*) | \bar{\chi}_c(s_1 \bar{n}) \Gamma \frac{\bar{n}}{2} \chi_c(0) | 0 \rangle = -\frac{if_{T\perp}(\mu)}{4} \bar{n} \cdot p_T \text{Tr} \left(\not{\varepsilon}_{\perp}^* \Gamma \frac{\not{n}\not{v}}{4} \right) \times \int_0^\infty du e^{ius_1 \bar{n} \cdot p_T} \phi_{T\perp}(u, \mu), \quad (41)$$

where ϕ_B and $\phi_{T\perp}$ are distribution amplitudes for B and T mesons, respectively. $f_{T\perp}$ is the decay constant of a tensor meson and it depends upon the scale of the theory. The scale dependent quantity $F(\mu)$ is related to B -meson decay constant f_B at NLO as

$$f_B \sqrt{m_B} = F(\mu) \left(1 + \frac{C_F \alpha_s(\mu)}{4\pi} \left(3 \ln \left(\frac{m_b}{\mu} \right) - 2 \right) \right).$$

Collecting the results from Eqs. (39, 40) and Eq. (41) to get the resummed matrix elements at leading power and at an order $\mathcal{O}(\alpha_s)$, we have

$$\begin{aligned} \mathcal{M} = \mathcal{C}^{\mathcal{A}}(E_F, \mu) \zeta_T^\perp(E_F) &= \frac{\sqrt{m_B}}{4} \left(\frac{2E_F}{\mu_Q} \right)^{a(\mu_Q, \mu_i)} e^{S(\mu_Q, \mu_i)} \int_0^\infty \frac{d\omega}{\omega} \phi_B(\omega, \mu) \int_0^1 du f_{T\perp} \phi_{T\perp}(u, v) \\ &\times \int_0^1 dv \mathcal{J}_\perp \left(u, v, \ln \frac{m_B \omega}{\mu^2} \right) U_\perp(u, v, \mu_Q, \mu_i) \mathcal{C}_1^{\mathcal{B}'}(v, \mu). \end{aligned} \quad (42)$$

The complete Wilson coefficients $C^{\mathcal{A}}$ and $C^{\mathcal{B}'}$ are given as

$$C^{\mathcal{A}} = \frac{G_F}{\sqrt{2}} V_{cp}^* V_{cb} \left[C_7 + \frac{C_F \alpha_s}{4\pi} (C_1 G_1(x_c) + C_8 G_8) \right] \nabla_7 C^{\mathcal{A}}, \quad (43)$$

$$C_1^{\mathcal{B}'} = \frac{G_F}{\sqrt{2}} V_{cp}^* V_{cb} \left[C_7 + C_1 \frac{1}{3} f \left(\frac{\bar{m}_c^2}{4\bar{u} E E_\gamma} \right) + C_8 \frac{\bar{u}}{3u} \right] \nabla_7 C^{\mathcal{B}'}, \quad (44)$$

where $p = s$ and d for K_2^* and (f_2, a_2) mesons, respectively. The function $G_1(x_c)$ and G_8 are given in Appendix 8. The LCDA for the tensor meson is defined as [10]

$$\phi_{T\perp} = 6u\bar{u} \left[1 + 3a_1^\perp \Upsilon + \frac{3}{2} a_2^\perp (5\Upsilon^2 - 1) \right], \quad (45)$$

with $\Upsilon = 2u - 1$ and it is normalized as $\int_0^1 \phi_\perp(u)/u = 1$. The Gegenbauer moments and decay constants are given in the Table 2. The distribution amplitudes for B -meson is a non-perturbative input heavily prone to uncertainty. Recent theoretical studies [38, 39] constrain the inverse B -moment (defined as $\lambda_B^{-1} = \int_0^\infty d\omega \Phi_B^+(\omega)$). In literature, [40, 41] the running of λ_B^{-1} is discussed. It is pertinent to mention that in principle one has to employ the RG evolution in the matching of SCET_I to SCET_{II} operators, and to do so one has to solve the one-loop SCET_{II} diagrams to find the corresponding anomalous dimension. But, due to the close values of intermediate scale $\mu_i \sim 1.5$ GeV and the hadronic scale, this is not required, and the values of decay constants and inverse B moment are taken at fixed value, i.e., 1 GeV just like the one in [23]. Therefore, here we took an optimal value of $\lambda_B^{-1} = 0.35 \pm 0.10 \text{ GeV}^{-1}$. The difference of the optimal value of $\lambda_B^+(1 \text{ GeV})$ we used here and the one given in [23] is due to the constraints discussed by Beneke *et al.* [38].

The soft overlap function, ζ_T^\perp , which is also the non-factorizable part and required as a nonperturbative input, is estimated from the form-factor values calculated in [11] by using Light-cone sum rules (LCSR). The seven form-factors for $B \rightarrow T$ can be related to ζ_T^\perp by invoking the heavy quark symmetry, therefore, to determine ζ_T^\perp at zero momentum transfer i.e., $q^2 = 0$, any one of them can be used [15]. Using this liberty, let us use the vector form-factor $V(q^2)$, which is calculated by using LCSR [9, 11], to determine the ζ_T^\perp , i.e.,

$$V(q^2) = \left(1 + \frac{m_T}{m_B} \right) \frac{E_F}{|\vec{p}_T|} C_{V1}^{\mathcal{A}} \zeta_T^\perp(E_F). \quad (46)$$

Here the Wilson Coefficient corresponding to a vector current at NLO is given as

$$C_{V1}^{\mathcal{A}} = 1 - \frac{\alpha_s C_F}{4\pi} \left[\left(\frac{1}{1-x} - 3 \right) \ln(x) + 2\ln^2(x) + 2\ln^2\left(\frac{\mu_Q}{m_b}\right)^2 + 2\text{Li}_2(1-x) - (4\ln(x) - 5)\ln\left(\frac{\mu_Q}{m_b}\right) + \frac{\pi^2}{12} + 6 \right] \quad (47)$$

The soft-overlap functions are thus calculated to be

$$\begin{aligned} \zeta_{K_2^*}^\perp(0) &= 0.295_{-0.056}^{+0.056}, \\ \zeta_{a_2}^\perp(0) &= 0.288_{-0.05}^{+0.06}, \\ \zeta_{f_2}^\perp(0) &= 0.185_{-0.08}^{+0.12}. \end{aligned} \quad (48)$$

The theoretical errors in the branching ratio of $B \rightarrow f_2 \gamma$ compared to the other two decays are higher due to the higher uncertainty in the value of the form-factor calculated in [11]. For consistency check, we also determined these soft overlap functions from the tensor current having an α_s

Branching ratios with a factor of 10^{-6} for $B \rightarrow (K_2^*, f_2, a_2)\gamma$ decays.				
Decay mode	(this work)	LFQM [12, 13]	HQET[14]	Experimental average[16]
$B \rightarrow K_2^*(1430)\gamma$	$16.7^{+6.36}_{-6.36} \pm 1.2$	$29.4^{+31.8}_{-13.9}$	21.8 ± 10.2	12.4 ± 2.4
$B \rightarrow a_2(1320)\gamma$	$0.67^{+0.30}_{-0.23} \pm 0.06$	—	—	—
$B \rightarrow f_2(1270)\gamma$	$0.18^{+0.23}_{-0.16} \pm 0.08$	—	—	—

Table 3: The results of branching ratios of $B \rightarrow (K_2^*, a_2, f_2)\gamma$ decays calculated in this work. In the case of $B \rightarrow K_2^*\gamma$, it is compared with the corresponding PDG averaged value, and with the values calculated using LFQM and HQET.

contribution, and found that they lie within 5% of the values found in Eq. (48). Comparing this value of the K_2^* with the corresponding overlap function for the K^* $\zeta_{K^*}^\perp = 0.37 \pm 0.04$ estimated from $B \rightarrow K^*\gamma$ [21] and $\zeta_{K^*}^\perp(q^2 = 0) = 0.32 \pm 0.02$ calculated from the semileptonic $B \rightarrow K^*$ decay [23], our result for $B \rightarrow K_2^*$ soft form-factor has comparatively large uncertainty coming from the LCSR calculation of the form-factor $V(q^2 = 0)$. The RG-improved branching ratios for $B \rightarrow (K_2^*, f_2, a_2)\gamma$ decays at NLO is given as

$$\mathcal{B}(B \rightarrow (K_2^*, f_2, a_2)\gamma) = \frac{\tau_B m_B}{4\pi} \left(1 + \frac{m_T^2}{8E_F |\vec{p}_T|}\right) \left(1 - \frac{m_T^2}{m_B^2}\right) |\mathcal{M}|^2, \quad (49)$$

Using these overlap functions, the branching ratios for $B \rightarrow (K_2^*, f_2, a_2)\gamma$ decays are calculated and these are given in Table (3). The first associated uncertainty is due to soft-overlap function while the second is the hadronic uncertainty coming from inverse B -moment and the decay constants. The dominant contribution to the branching fraction is due to the first term in the amplitude Eq. (42), which we can call as the soft-amplitude ($\mathcal{M}_{\text{soft}}$) while the second term in (42) may be termed as hard-amplitude ($\mathcal{M}_{\text{hard}}$). The contribution of $\mathcal{M}_{\text{hard}}$ to the total branching ratio of $B \rightarrow K_2^*\gamma$ is 26% of the value of the lone contribution from $\mathcal{M}_{\text{soft}}$. The hard-amplitude is itself RG-improved and induces 6.5% correction to the branching ratio compared to the one without RG-improvement. For $B \rightarrow K_2^*\gamma$, our result of the branching ratio is compared with the values calculated using LFQM [12, 13], HQET [14] and the experimental measured averaged value [16]. Our result (although prone to uncertainty) is closer to the experimental average. The branching ratio is very sensitive to the soft-overlap function and its precise measurement reduces the uncertainties significantly.

7 Conclusion

The rare radiative $B \rightarrow K^*$ decays were studied using HQET/LEET and SCET [18, 29]. By changing the final state vector mesons with the corresponding axial-vector meson ($J^P = 1^+$), the branching ratios of $B \rightarrow (K_1, b_1, a_1)\gamma$ decays in the SECT are found in [8]. In this work, we employed SCET to calculate the branching ratio of the radiative B to tensor meson decays, i.e., $B \rightarrow (K_2^*, f_2, a_2)\gamma$ at NLO in strong coupling constant (α_s) and at leading power of $1/m_b$. The QCD diagrams matched with SCET_I at the loop (tree) level for $\mathcal{A}(\mathcal{B}')$ - type operators. For the \mathcal{B}' - type operators, we resummed the large logarithms using the one loop diagrams for the SCET_I. Using the value of soft form factor (soft-overlap function) estimated using LCSR approach [11], we calculated the branching ratios for $B \rightarrow (K_2^*, f_2, a_2)\gamma$ decays. We found that our result (central value) of the branching ratio of $B \rightarrow K_2^*\gamma$ are smaller than the corresponding LFQM [12, 13] and HQET [14], but closer to the PDG experimental average [16]. The other important feature of the calculation done here is that the errors in the branching ratio of $B \rightarrow K_2^*\gamma$ are small compared to [12, 13, 14], because we used LCSR value of $V(q^2 = 0)$ having small uncertainties to extract

soft-overlap function (ζ_T^\perp). In contrast with $B \rightarrow K_2^* \gamma$, the branching ratios of $B \rightarrow (a_2, f_2) \gamma$ are CKM suppressed, and we hope that these would be measured in some ongoing and future B physics experiments.

8 Appendix

For the matching of Q_1 and Q_8 on \mathcal{A} -type operators, the functions G_1 and G_8 were required. These are taken from [42], and their explicit form is

$$\begin{aligned}
G_1(x) &= \frac{-104}{27} \ln \frac{\mu}{m_b} - \frac{833}{162} - \frac{20\pi i}{27} + 8 \frac{8\pi^2}{9} x^{3/2} \\
&+ \frac{2}{9} \left[48 + 30\pi i - 5\pi^2 - 36\xi(3) + (36 + 6\pi i - 9\pi^2) \ln(x) + (3 + 6\pi i) (\ln(x))^2 + (\ln(x))^3 \right] x \\
&+ \frac{2}{9} \left[18 + 2\pi^2 - 2\pi^3 + (12 - 6\pi^2) \ln x + 6\pi i (\ln(x))^2 + (\ln(x))^3 \right] x^2 \\
&+ \frac{1}{27} \left[-9 + 112\pi i - 14\pi^2 + (182 - 48\pi i) \ln(x) - 126 (\ln(x))^2 \right] x^3 + \mathcal{O}(x^4), \\
G_8 &= \frac{8}{3} \ln \left(\frac{\mu}{m_b} \right) + \frac{11}{3} + \frac{2\pi i}{3} - \frac{2\pi^2}{9},
\end{aligned} \tag{50}$$

here $x = m_c^2/m_b^2$. The function $f(z)$, where $z = \frac{m_q^2}{4EE_\gamma u}$, given in the matching of Q_1 operators to \mathcal{B}' and \mathcal{C} -types currents is

$$f(z) = \begin{cases} 1 + 4z \left(\operatorname{arctanh}(\sqrt{1-4z}) - i\frac{\pi}{2} \right)^2, & \text{for } z < 1/4 \\ 1 - 4z \arctan^2 \frac{1}{\sqrt{4z-1}}, & \text{for } z > 1/4. \end{cases} \tag{51}$$

References

- [1] M. Misiak, H. Asatrian, R. Boughezal, M. Czakon, T. Ewerth, A. Ferroglia, P. Fiedler, P. Gambino, C. Greub, U. Haisch, T. Huber, M. Kaminski, G. Ossola, M. Poradzinski, A. Rehman, T. Schutzmeier, M. Steinhauser and J. Virto, Phys. Rev. Lett. **114**, no.22, 221801 (2015) doi:10.1103/PhysRevLett.114.221801 [arXiv:1503.01789 [hep-ph]].
- [2] P. Ball, G. W. Jones and R. Zwicky, Phys. Rev. D **75**, 054004 (2007) doi:10.1103/PhysRevD.75.054004 [arXiv:hep-ph/0612081 [hep-ph]].
- [3] R. N. Faustov and V. O. Galkin, Mod. Phys. Lett. A **7**, 2111-2117 (1992) doi:10.1142/S0217732392001853
- [4]
- [4] A. Khodjamirian, T. Mannel, A. A. Pivovarov and Y. M. Wang, JHEP **09** (2010), 089 doi:10.1007/JHEP09(2010)089 [arXiv:1006.4945 [hep-ph]].
- [5] N. Oshimo, Nucl. Phys. B **404**, 20-41 (1993) doi:10.1016/0550-3213(93)90471-Z
- [6] M. Jung, X. Q. Li and A. Pich, JHEP **10**, 063 (2012) doi:10.1007/JHEP10(2012)063 [arXiv:1208.1251 [hep-ph]].
- [7] A. Sikandar, M. J. Aslam, I. Ahmed and S. Shafaq, Phys. Rev. D **100**, no.5, 056013 (2019) doi:10.1103/PhysRevD.100.056013 [arXiv:1909.04384 [hep-ph]].

- [8] A. Sikandar, M. J. Aslam, I. Ahmed and S. Shafaq, J. Phys. G **48** (2021) no.4, 045005 doi:10.1088/1361-6471/abdadd
- [9] W. Wang, Phys. Rev. D **83**, 014008 (2011) doi:10.1103/PhysRevD.83.014008 [arXiv:1008.5326 [hep-ph]].
- [10] K. C. Yang, Phys. Lett. B **695**, 444-448 (2011) doi:10.1016/j.physletb.2010.11.053 [arXiv:1010.2944 [hep-ph]].
- [11] T. M. Aliev, H. Dag, A. Kokulu and A. Ozpineci, Phys. Rev. D **100**, no.9, 094005 (2019) doi:10.1103/PhysRevD.100.094005 [arXiv:1908.00847 [hep-ph]].
- [12] H. Y. Cheng, C. K. Chua and C. W. Hwang, Phys. Rev. D **69**, 074025 (2004) doi:10.1103/PhysRevD.69.074025 [arXiv:hep-ph/0310359 [hep-ph]].
- [13] H. Y. Cheng and C. K. Chua, Phys. Rev. D **81**, 114006 (2010) [erratum: Phys. Rev. D **82**, 059904 (2010)] doi:10.1103/PhysRevD.81.114006 [arXiv:0909.4627 [hep-ph]].
- [14] S. Veseli and M. G. Olsson, Phys. Lett. B **367**, 309-316 (1996) doi:10.1016/0370-2693(95)01408-X [arXiv:hep-ph/9508255 [hep-ph]].
- [15] A. Sikandar, M. J. Aslam, I. Ahmed and S. Shafaq, J. Phys. G **49** (2022) no.10, 105002 doi:10.1088/1361-6471/ac8567
- [16] R. L. Workman *et al.* [Particle Data Group], PTEP **2022**, 083C01 (2022) doi:10.1093/ptep/ptac097
- [17] C.W. Bauer, D. Pirjol, I.W. Stewart, Phys. Rev. D **67**(2003)071502, hep-ph/0206152.
- [18] M. Beneke and T. Feldmann, Nucl. Phys. B **685**, 249-296 (2004) doi:10.1016/j.nuclphysb.2004.02.033 [arXiv:hep-ph/0311335 [hep-ph]].
- [19] B. O. Lange and M. Neubert, Nucl. Phys. B **690**, 249-278 (2004) [erratum: Nucl. Phys. B **723**, 201-202 (2005)] doi:10.1016/j.nuclphysb.2005.06.019 [arXiv:hep-ph/0311345 [hep-ph]].
- [20] J. Charles, A. Le Yaouanc, L. Oliver, O. Pene and J. Raynal, Phys. Rev. D **60**, 014001 (1999) doi:10.1103/PhysRevD.60.014001 [arXiv:hep-ph/9812358 [hep-ph]].
- [21] T. Becher, R. J. Hill and M. Neubert, Phys. Rev. D **72**, 094017 (2005) doi:10.1103/PhysRevD.72.094017 [hep-ph/0503263].
- [22] R. J. Hill, T. Becher, S. J. Lee and M. Neubert, JHEP **0407**, 081 (2004) doi:10.1088/1126-6708/2004/07/081 [hep-ph/0404217].
- [23] A. Ali, G. Kramer and G. h. Zhu, Eur. Phys. J. C **47** (2006), 625-641 doi:10.1140/epjc/s2006-02596-4 [arXiv:hep-ph/0601034 [hep-ph]].
- [24] C. Bobeth, M. Misiak and J. Urban, Nucl. Phys. B **574**, 291 (2000) doi:10.1016/S0550-3213(00)00007-9 [hep-ph/9910220].
- [25] M. Gorbahn, U. Haisch and M. Misiak, Phys. Rev. Lett. **95**, 102004 (2005) doi:10.1103/PhysRevLett.95.102004 [arXiv:hep-ph/0504194 [hep-ph]].
- [26] M. Czakon, U. Haisch and M. Misiak, JHEP **0703**, 008 (2007) doi:10.1088/1126-6708/2007/03/008 [hep-ph/0612329].

- [27] T. Blake, G. Lanfranchi and D. M. Straub, *Prog. Part. Nucl. Phys.* **92**, 50-91 (2017) doi:10.1016/j.pnpnp.2016.10.001 [arXiv:1606.00916 [hep-ph]].
- [28] D. Ebert, R. N. Faustov and V. O. Galkin, *Phys. Rev. D* **64** (2001), 094022 doi:10.1103/PhysRevD.64.094022 [arXiv:hep-ph/0107065 [hep-ph]].
- [29] T. Becher, R. J. Hill and M. Neubert, *Phys. Rev. D* **69**, 054017 (2004) doi:10.1103/PhysRevD.69.054017 [arXiv:hep-ph/0308122 [hep-ph]].
- [30] M. Beneke, Y. Kiyo and D. S. Yang, *Nucl. Phys. B* **692**, 232 (2004) doi:10.1016/j.nuclphysb.2004.05.018 [hep-ph/0402241].
- [31] M. Beneke, *Nucl. Part. Phys. Proc.* **261-262**, 311-337 (2015) doi:10.1016/j.nuclphysbps.2015.03.021 [arXiv:1501.07374 [hep-ph]].
- [32] C. W. Bauer, S. Fleming, D. Pirjol and I. W. Stewart, *Phys. Rev. D* **63**, 114020 (2001) doi:10.1103/PhysRevD.63.114020 [hep-ph/0011336].
- [33] C. Greub, T. Hurth and D. Wyler, *Phys. Rev. D* **54**, 3350 (1996) doi:10.1103/PhysRevD.54.3350 [hep-ph/9603404].
- [34] J. Chay and C. Kim, *Phys. Rev. D* **68**, 034013 (2003) doi:10.1103/PhysRevD.68.034013 [arXiv:hep-ph/0305033 [hep-ph]].
- [35] S. Descotes-Genon and C. Sachrajda, *Nucl. Phys. B* **693**, 103-133 (2004) doi:10.1016/j.nuclphysb.2004.06.018 [arXiv:hep-ph/0403277 [hep-ph]].
- [36] S. Bosch, R. Hill, B. Lange and M. Neubert, *Phys. Rev. D* **67**, 094014 (2003) doi:10.1103/PhysRevD.67.094014 [arXiv:hep-ph/0301123 [hep-ph]].
- [37] S. Aoki *et al.* [Flavour Lattice Averaging Group], *Eur. Phys. J. C* **80**, no.2, 113 (2020) doi:10.1140/epjc/s10052-019-7354-7 [arXiv:1902.08191 [hep-lat]].
- [38] M. Beneke and J. Rohrwild, *Eur. Phys. J. C* **71**, 1818 (2011) doi:10.1140/epjc/s10052-011-1818-8 [arXiv:1110.3228 [hep-ph]].
- [39] Y. M. Wang, *JHEP* **09**, 159 (2016) doi:10.1007/JHEP09(2016)159 [arXiv:1606.03080 [hep-ph]].
- [40] Y. M. Wang and Y. L. Shen, *Nucl. Phys. B* **898** (2015), 563-604 doi:10.1016/j.nuclphysb.2015.07.016 [arXiv:1506.00667 [hep-ph]].
- [41] J. Gao, C. D. Lü, Y. L. Shen, Y. M. Wang and Y. B. Wei, *Phys. Rev. D* **101** (2020) no.7, 074035 doi:10.1103/PhysRevD.101.074035 [arXiv:1907.11092 [hep-ph]].
- [42] S. W. Bosch and G. Buchalla, *Nucl. Phys. B* **621**, 459 (2002) doi:10.1016/S0550-3213(01)00580-6 [hep-ph/0106081].